

Observation of $B \rightarrow J/\psi K_1(1270)$

The Belle Collaboration

K. Abe¹⁰, K. Abe³⁸, I. Adachi¹⁰, Byoung Sup Ahn¹⁶, H. Aihara⁴⁰, M. Asai¹¹, Y. Asano⁴⁵, T. Aso⁴⁴, V. Aulchenko², T. Aushev¹⁴, A. M. Bakich³⁶, E. Banas²⁶, W. Bartel^{6,10}, S. Behari¹⁰, P. K. Behera⁴⁶, D. Beilina², A. Bondar², A. Bozek²⁶, T. E. Browder⁹, B. C. K. Casey⁹, P. Chang²⁵, Y. Chao²⁵, B. G. Cheon³⁵, S.-K. Choi⁸, Y. Choi³⁵, J. Dragic¹⁹, A. Drutskoy¹⁴, S. Eidelman², Y. Enari²¹, F. Fang⁹, H. Fujii¹⁰, C. Fukunaga⁴², M. Fukushima¹², A. Garmash^{2,10}, A. Gordon¹⁹, K. Gotow⁴⁷, R. Guo²³, J. Haba¹⁰, H. Hamasaki¹⁰, K. Hanagaki³², K. Hara³⁰, T. Hara³⁰, N. C. Hastings¹⁹, H. Hayashii²², M. Hazumi³⁰, E. M. Heenan¹⁹, Y. Higashino²¹, I. Higuchi³⁹, T. Higuchi⁴⁰, H. Hirano⁴³, T. Hojo³⁰, Y. Hoshi³⁸, S.-R. Hou²⁵, W.-S. Hou²⁵, S.-C. Hsu²⁵, H.-C. Huang²⁵, Y. Igarashi¹⁰, T. Iijima¹⁰, H. Ikeda¹⁰, K. Inami²¹, A. Ishikawa²¹, H. Ishino⁴¹, R. Itoh¹⁰, G. Iwai²⁸, H. Iwasaki¹⁰, Y. Iwasaki¹⁰, D. J. Jackson³⁰, P. Jalocho²⁶, H. K. Jang³⁴, M. Jones⁹, R. Kagan¹⁴, H. Kakuno⁴¹, J. Kaneko⁴¹, J. H. Kang⁴⁸, J. S. Kang¹⁶, P. Kapusta²⁶, N. Katayama¹⁰, H. Kawai³, H. Kawai⁴⁰, N. Kawamura¹, T. Kawasaki²⁸, H. Kichimi¹⁰, D. W. Kim³⁵, Heejong Kim⁴⁸, H. J. Kim⁴⁸, Hyunwoo Kim¹⁶, S. K. Kim³⁴, T. H. Kim⁴⁸, K. Kinoshita⁵, S. Kobayashi³³, S. Koishi⁴¹, P. Krokovny², R. Kulasiri⁵, S. Kumar³¹, A. Kuzmin², Y.-J. Kwon⁴⁸, J. S. Lange⁷, S. H. Lee³⁴, D. Liventsev¹⁴, R.-S. Lu²⁵, D. Marlow³², T. Matsubara⁴⁰, S. Matsui²¹, S. Matsumoto⁴, T. Matsumoto²¹, Y. Mikami³⁹, K. Miyabayashi²², H. Miyake³⁰, H. Miyata²⁸, G. R. Moloney¹⁹, G. F. Moorhead¹⁹, S. Mori⁴⁵, T. Mori⁴, A. Murakami³³, T. Nagamine³⁹, Y. Nagasaka¹¹, Y. Nagashima³⁰, T. Nakadaira⁴⁰, E. Nakano²⁹, M. Nakao¹⁰, J. W. Nam³⁵, S. Narita³⁹, Z. Natkaniec²⁶, K. Neichi³⁸, S. Nishida¹⁷, O. Nitoh⁴³, S. Noguchi²², T. Nozaki¹⁰, S. Ogawa³⁷, T. Ohshima²¹, T. Okabe²¹, S. Okuno¹⁵, S. L. Olsen⁹, H. Ozaki¹⁰, P. Pakhlov¹⁴, H. Palka²⁶, C. S. Park³⁴, C. W. Park¹⁶, H. Park¹⁸, L. S. Peak³⁶, M. Peters⁹, L. E. Piilonen⁴⁷, E. Prebys³², J. L. Rodriguez⁹, N. Root², M. Rozanska²⁶, K. Rybicki²⁶, H. Sagawa¹⁰, Y. Sakai¹⁰, H. Sakamoto¹⁷, M. Satpathy⁴⁶, A. Satpathy^{10,5}, S. Schrenk⁵, S. Semenov¹⁴, K. Senyo²¹, M. E. Sevir¹⁹, H. Shibuya³⁷, B. Shwartz², S. Stanić⁴⁵, A. Sugi²¹, A. Sugiyama²¹, K. Sumisawa¹⁰, T. Sumiyoshi¹⁰, J.-I. Suzuki¹⁰, K. Suzuki³, S. Suzuki^{21,*}, S. Y. Suzuki¹⁰, S. K. Swain⁹, T. Takahashi²⁹, F. Takasaki¹⁰, M. Takita³⁰, K. Tamai¹⁰, N. Tamura²⁸, J. Tanaka⁴⁰, M. Tanaka¹⁰, Y. Tanaka²⁰, G. N. Taylor¹⁹, Y. Teramoto²⁹, M. Tomoto¹⁰, T. Tomura⁴⁰, S. N. Tovey¹⁹, K. Trabelsi⁹, T. Tsuboyama¹⁰, T. Tsukamoto¹⁰, S. Uehara¹⁰, K. Ueno²⁵, Y. Unno³, S. Uno¹⁰, Y. Ushiroda¹⁰, S. E. Vahsen³², K. E. Varvell³⁶, C. H. Wang²⁴, J. G. Wang⁴⁷, M.-Z. Wang²⁵, Y. Watanabe⁴¹, E. Won³⁴, B. D. Yabsley¹⁰, Y. Yamada¹⁰, M. Yamaga³⁹, A. Yamaguchi³⁹, H. Yamamoto⁹, Y. Yamashita²⁷, M. Yamauchi¹⁰, S. Yanaka⁴¹, K. Yoshida²¹, Y. Yusa³⁹, H. Yuta¹, C. C. Zhang¹³, J. Zhang⁴⁵, H. W. Zhao¹⁰, Y. Zheng⁹, V. Zhilich², and D. Žontar⁴⁵

¹*Aomori University, Aomori*

²*Budker Institute of Nuclear Physics, Novosibirsk*

³*Chiba University, Chiba*

⁴*Chuo University, Tokyo*

⁵*University of Cincinnati, Cincinnati, OH*

⁶*Deutsches Elektronen-Synchrotron, Hamburg*

⁷*University of Frankfurt, Frankfurt*

⁸*Gyeongsang National University, Chinju*

⁹*University of Hawaii, Honolulu HI*

¹⁰*High Energy Accelerator Research Organization (KEK), Tsukuba*

¹¹*Hiroshima Institute of Technology, Hiroshima*

¹²*Institute for Cosmic Ray Research, University of Tokyo, Tokyo*

¹³*Institute of High Energy Physics, Chinese Academy of Sciences, Beijing*

¹⁴*Institute for Theoretical and Experimental Physics, Moscow*

¹⁵*Kanagawa University, Yokohama*

¹⁶*Korea University, Seoul*

¹⁷*Kyoto University, Kyoto*

¹⁸*Kyungpook National University, Taegu*

¹⁹*University of Melbourne, Victoria*

²⁰*Nagasaki Institute of Applied Science, Nagasaki*

²¹*Nagoya University, Nagoya*

²²*Nara Women's University, Nara*

²³*National Kaohsiung Normal University, Kaohsiung*

²⁴*National Lien-Ho Institute of Technology, Miao Li*

²⁵*National Taiwan University, Taipei*

²⁶*H. Niewodniczanski Institute of Nuclear Physics, Krakow*

- ²⁷ *Nihon Dental College, Niigata*
²⁸ *Niigata University, Niigata*
²⁹ *Osaka City University, Osaka*
³⁰ *Osaka University, Osaka*
³¹ *Panjab University, Chandigarh*
³² *Princeton University, Princeton NJ*
³³ *Saga University, Saga*
³⁴ *Seoul National University, Seoul*
³⁵ *Sungkyunkwan University, Suwon*
³⁶ *University of Sydney, Sydney NSW*
³⁷ *Toho University, Funabashi*
³⁸ *Tohoku Gakuin University, Tagajo*
³⁹ *Tohoku University, Sendai*
⁴⁰ *University of Tokyo, Tokyo*
⁴¹ *Tokyo Institute of Technology, Tokyo*
⁴² *Tokyo Metropolitan University, Tokyo*
⁴³ *Tokyo University of Agriculture and Technology, Tokyo*
⁴⁴ *Toyama National College of Maritime Technology, Toyama*
⁴⁵ *University of Tsukuba, Tsukuba*
⁴⁶ *Utkal University, Bhubaneswer*
⁴⁷ *Virginia Polytechnic Institute and State University, Blacksburg VA*
⁴⁸ *Yonsei University, Seoul*
* *Now at Yokkaichi University*
(October 31, 2018)

We report the first observation of the exclusive decay process $B \rightarrow J/\psi K_1(1270)$ using a sample of 11.2M $B\bar{B}$ meson pairs collected in the Belle detector at the KEKB asymmetric energy e^+e^- collider. We measure branching fractions of $\mathcal{B}(B^0 \rightarrow J/\psi K_1^0(1270)) = (1.30 \pm 0.34 \pm 0.31) \times 10^{-3}$ and $\mathcal{B}(B^+ \rightarrow J/\psi K_1^+(1270)) = (1.80 \pm 0.34 \pm 0.39) \times 10^{-3}$, where the first error is statistical and the second is systematic. These modes constitute approximately 15% of the total number of $B \rightarrow J/\psi X$ decays. No evidence is seen for $B \rightarrow J/\psi K_1(1400)$ and we set an upper limit for this branching fraction. The $K_1(1270) \rightarrow K^0 \pi^+ \pi^-$ decays have a substantial $K^0 \rho^0$ intermediate state component that may be useful for CP violation studies.

PACS numbers:11.30.Er,12.15.Hh,13.25.Hw

Decays of B mesons into final states containing the J/ψ charmonium state play a special role in studies of CP violation physics. Since the J/ψ is itself a CP eigenstate, final states where the accompanying particles are matter-antimatter symmetric are potentially useful for CP violation measurements. Moreover, these decay modes are experimentally convenient, primarily because the $J/\psi \rightarrow \ell^+\ell^-$ ($\ell^+\ell^- = e^+e^-$ or $\mu^+\mu^-$) final states have a rather distinct signature.

However, although the branching fraction for inclusive $B \rightarrow J/\psi X$ decay is relatively large ($\sim 1\%$), only a small fraction of these decays have been associated with exclusive decay modes that are relevant for CP studies. Since all current experimental searches for CP violations in B meson decays are statistics limited, it is important to identify additional decay modes that might be useful. Decays of the type $B^0 \rightarrow J/\psi K_1^0(1270)$ are of interest because the $K_1^0(1270)$ has an appreciable branching fraction to the *flavor-nonspecific* $K^0\rho^0$ final state (14%) and, thus, might be useful for CP measurements. At present there is very little experimental information available about any exclusive $B \rightarrow J/\psi K\pi\pi$ decay modes [1].

In this Letter we describe a study of the $B \rightarrow J/\psi K\pi\pi$ decay process using the Belle detector [2] at the KEKB asymmetric energy e^+e^- storage ring [3]. We observe a signal for exclusive decays where the properties of the $K\pi\pi$ system are consistent with those of the $K_1(1270)$ resonance. The data sample corresponds to an integrated luminosity of 10.5 fb^{-1} accumulated at the $\Upsilon(4S)$ resonance and contains $11.2M \overline{B}B$ meson pairs.

The Belle detector consists of a three-layer silicon vertex detector, a 50-layer central drift chamber (CDC) for charged particle tracking and specific ionization measurements (dE/dx), an array of 1188 aerogel Čerenkov counters (ACC), a time-of-flight (TOF) system comprised of 128 scintillation counters, and an electromagnetic calorimeter containing 8736 CsI(Tl) crystals (ECL), all located inside a 3.4 m diameter superconducting solenoid that generates a 1.5 Tesla magnetic field. An iron flux-return yoke outside the solenoid is comprised of 14 layers of 4.7 cm-thick iron plates interleaved with a system of resistive plate counters (KLM) that are used for muon identification and K_L detection. Electron identification is based on a combination of CDC dE/dx information, the response of the ACC, and the position, shape and energy deposit of the associated ECL shower. Muon identification relies on the location and penetration depth of associated tracks in the KLM. We use a Monte Carlo (MC) simulation to model the response of the detector and determine acceptances [4]. The detector is described in detail in ref. [2].

We select events with three final state topologies: $B^+ \rightarrow J/\psi K^+\pi^+\pi^-$, and $B^0 \rightarrow J/\psi K^+\pi^-\pi^0$ and $J/\psi K^0\pi^+\pi^-$, where $J/\psi \rightarrow \ell^+\ell^-$ and $K^0 \rightarrow \pi^+\pi^-$. We use $B^+ \rightarrow J/\psi K^+$ decays for normalization. (Here, as in the rest of this report, inclusion of the charge con-

jugate states is implied.) Candidate $J/\psi \rightarrow \mu^+\mu^-$ decays are oppositely charged track pairs where at least one track is positively identified as a muon and the other is either positively identified as a muon or has an associated ECL energy deposit that is consistent with a minimum ionizing particle. The invariant mass of the candidate $\mu^+\mu^-$ pair is required to be within $\pm 3\sigma$ of the J/ψ mass peak, where $\sigma \simeq 12 \text{ MeV}$ is the mass resolution. Candidate $J/\psi \rightarrow e^+e^-$ decays are oppositely charged track pairs where at least one track is well identified as an electron and the other track satisfies at least either the dE/dx or the ECL electron identification requirements. In this channel, we partially correct for final state radiation or real bremsstrahlung in the inner parts of the detector by including the four-momentum of every photon detected within 0.05 radians of the original e^+ or e^- direction in the e^+e^- invariant mass calculation. Since the $J/\psi \rightarrow e^+e^-$ peak still has a residual radiative tail, we use an asymmetric invariant mass requirement $-7\sigma \leq (M_{e^+e^-} - M_{J/\psi}) \leq 3\sigma$ ($\sigma \simeq 12 \text{ MeV}$). After selection, the J/ψ candidate tracks are refitted to a common vertex and then mass constrained to $M_{J/\psi}$. The fitted vertex is then used as the vertex point of reference for the other particles in the decay.

For charged hadron identification we use the combination of CDC dE/dx measurements, flight times measured in the TOF, and the response of the ACC to determine a relative K/π discrimination variable that ranges from $\mathcal{P}_{K/\pi} = 0$ for unambiguous pions, to $\mathcal{P}_{K/\pi} = 1$ for well identified kaons. In this analysis we identify charged tracks with $\mathcal{P}_{K/\pi} > 0.5$ as kaons and those with $\mathcal{P}_{K/\pi} \leq 0.5$ as pions. For $\pi^0 \rightarrow \gamma\gamma$ candidates, we require a minimum γ energy of 40 MeV and use $\gamma\gamma$ pairs with a total laboratory energy greater than 230 MeV and an invariant mass that is within $\pm 2\sigma$ of M_{π^0} , where the average value of σ is 4.9 MeV. For $K^0 \rightarrow \pi^+\pi^-$, we use oppositely charged track pairs where the two-track vertex is displaced from that of the J/ψ in the transverse ($r-\phi$) plane by more than 0.8 mm, the ϕ directions of the vertex point and the K^0 candidate's three momentum vector agree within 0.2 radians, and the $\pi^+\pi^-$ invariant mass is within $\pm 3\sigma$ of M_{K^0} , where $\sigma \simeq 4 \text{ MeV}$. We eliminate events of the type $B^+ \rightarrow \psi(2S)K^+$, where $\psi(2S) \rightarrow \pi^+\pi^-J/\psi$, by requiring $M_{\pi\pi\ell\ell} - M_{\ell\ell}$ to differ from $M_{\psi(2S)} - M_{J/\psi}$ by more than $\pm 9 \text{ MeV}$ (3σ).

Candidate B mesons are identified by their center of mass (cm) energy difference, $\Delta E = \sum_i E_i - E_b$, and the beam constrained mass, $M_{bc} = \sqrt{E_b^2 - (\sum_i \vec{p}_i)^2}$, where $E_b = \sqrt{s}/2$ is the beam energy in the cm frame and \vec{p}_i and E_i are the cm three-momenta and energies of the candidate B meson decay products. We select events with $M_{bc} > 5.25 \text{ GeV}$ and $|\Delta E| < 0.2 \text{ GeV}$, and define a $\pm 3\sigma$ signal window of $|M_{bc} - M_B| < 9 \text{ MeV}$ and $|\Delta E| < 60 \text{ MeV}$ and an equal area *sideband* region that corresponds to the same M_{bc} selection and

60 MeV < $\Delta E \leq 180$ MeV [5].

About 10% of selected events have more than one entry in the $M_{bc} > 5.25$ GeV and $|\Delta E| < 0.2$ GeV region. Multiple entries from additional charged pions are primarily due to extra tracks produced by low momentum curling particles ($p_t < 0.25$ GeV/c); fake π^0 s are due to low energy γ combinatoric background. For multiple charged track entries, we select the one with the smallest impact parameter relative to the refitted J/ψ vertex. According to the MC simulation, these criteria select the correct track in 75% of the cases. For multiple entries involving π^0 candidates, we chose the $\gamma\gamma$ combination with an invariant mass closest to M_{π^0} . This selects the correct $\gamma\gamma$ combination in 60% of the cases.

Figure 1(a) shows the distribution of $M_{\pi^+\pi^-}$ vs $M_{K^+\pi^+\pi^-}$ for events in the M_{bc} and ΔE signal window. The clustering near $M_{\pi\pi} \simeq M_\rho$ and $M_{K\pi\pi} \simeq 1.27$ GeV is consistent with expectations for $K_1(1270) \rightarrow K\rho$ decays. In these decays, the $K\pi\pi$ and $\pi\pi$ systems are produced very near the kinematic boundary, which distorts the resonance line shapes for both the ρ and the $K_1(1270)$. Figure 1(b) shows the $M_{K^+\pi^+\pi^-}$ distribution for the events with -150 MeV < $(M_{\pi\pi} - M_\rho) < 50$ MeV [6]. In the figure, the clear histogram represents the events in the M_{bc} vs. ΔE signal window; sideband region events are shown as the cross-hatched histogram. The lower curve shows the result of a fit to a phase-space-like background function to the sideband $M_{K\pi\pi}$ distribution. The upper curve shows the results of a fit to the mass region below 1.7 GeV that uses the background determined from the sideband distribution plus a line shape function that was specialized [7] to expectations for $K_1 \rightarrow K\rho$ decays with the PDG values for the K_1 mass and total width used as input [8]. The sideband background plus the $K_1(1270)$ line shape function, which has only its normalization as a free parameter, gives a good fit to the lower part of the $K\pi\pi$ mass spectrum [9], indicating that our interpretation of the event cluster in Fig. 1(a) as being due to the $K_1(1270)$ is reasonable.

In flavor-SU(3), the strange axial-vector eigenstates are mixtures of the $K_1(1270)$ with the $K_1(1400)$, which decays primarily via $K^*(890)\pi$ (Bf \simeq 94%). We searched the same events for a $K_1(1400)$ signal in the distribution of $M_{K^+\pi^-}$ vs $M_{K^+\pi^+\pi^-}$ shown in Fig. 1(c). Here there is no obvious concentration of events around $M_{K\pi} \simeq M_{K^*}$ and $M_{K\pi\pi} \simeq M_{K_1(1400)}$. Figure 1(d) shows the $M_{K\pi\pi}$ projection for events with $|M_{K\pi} - M_{K^*}| < 50$ MeV, where again there is no evidence for a $K_1(1400)$ signal; the $M_{K\pi\pi} < 1.7$ GeV mass region is well fitted by a sideband background plus the $K_1(1270)$.

We select $B \rightarrow J/\psi K_1(1270)$ candidate events as those that satisfy the ρ mass requirements and have 1.16 GeV $\leq M_{K\pi\pi} \leq 1.38$ GeV. The MC simulation indicates that this mass window accepts 41% of all $K_1(1270) \rightarrow K\pi\pi$ decays.

Figures 2(a) through 2(f) show, alternately, the pro-

jections of the M_{bc} and ΔE signal bands for the selected $B \rightarrow J/\psi K_1(1270)$ candidates in the $J/\psi K^+\pi^+\pi^-$, $J/\psi K^+\pi^-\pi^0$, and $J/\psi K^0\pi^+\pi^-$ channels, respectively. The M_{bc} distributions are for events with $|\Delta E| < 0.06$ GeV, and the ΔE distributions are for events with $M_{bc} > 5.271$ GeV. The curve in each figure is the result of a simultaneous fit to the M_{bc} and ΔE projections where the two distributions are fitted with Gaussian signal functions that are constrained to have the same number of events. For the M_{bc} projection, we parameterize the background with a function that behaves like phase space near the endpoint; for ΔE , we represent the background with a linear function and restrict the fit to the range -0.1 GeV < ΔE < $+0.2$ GeV [5]. The widths of the M_{bc} distributions are primarily due to the cm energy spread and are expected to be nearly the same for each channel; in the fits we fix them at the value $\sigma_{M_{bc}} = 3.0$ MeV, which is determined from $B^0 \rightarrow J/\psi K_S^0$ events in the same data sample [10]. For the fits to the $K^+\pi^+\pi^-$ channel, the values of the signal peak positions and the ΔE width are free parameters; the fit results are consistent with MC expectations. In the $K^+\pi^-\pi^0$ and $K^0\pi^+\pi^-$ channels, where the statistics are limited, the signal peak positions and widths are fixed at their expected values.

We use the $B^+ \rightarrow J/\psi K^+$ events from the same data sample for normalization. We select these events using the same J/ψ and charged kaon criteria as used in the $B \rightarrow J/\psi K\pi\pi$ selection. The number of events are extracted using the same fitting procedure. The yields from the fits for all channels are listed in Table I.

We searched for a $B^+ \rightarrow J/\psi K_1^+(1400)$ signal using selection requirements optimized for $K_1^+(1400) \rightarrow K^{*0}\pi^+ \rightarrow K^+\pi^+\pi^-$, namely $|M_{K\pi} - M_{K^*}| < 50$ MeV and $|M_{K\pi\pi} - M_{K_1(1400)}| < 175$ MeV. In this case the signal observed is consistent with the contribution from the tail of the $K_1(1270)$. (There is about a 40% overlap between the $K_1(1270)$ and the $K_1(1400)$ selection requirements.) We determine an acceptance-corrected ratio of the event yield $N_{ev}[B^+ \rightarrow J/\psi K_1^+(1400)]/N_{ev}[B^+ \rightarrow J/\psi K_1^+(1270)] = 0.07 \pm 0.14$ from which we conclude that contributions to the $K_1(1270)$ signal from the $K_1(1400)$ resonance are less than 9% (at the 1σ level).

The number of $K_1^+(1270)$ events in the $\pi^+\pi^-$ vs $K^+\pi^+\pi^-$ mass window, determined from the fit to the $M_{K\pi\pi}$ distribution shown in Fig. 1(b), is 53.2 ± 10.0 events, which is very nearly the same as the number of signal events determined from the simultaneous fits to the ΔE and M_b projections (53.4 events). From this agreement, we rule out more than a 7% non-resonant $K\pi\pi$ component to our observed signal (at the 1σ level).

We determine the ratio of branching fractions using MC-determined acceptances and K_1 branching fractions to the accepted topologies that are taken from the PDG tables [8]. Here we assume the ratio of charged to neutral B meson production at the $\Upsilon(4S)$ is unity. The results

for the two neutral K_1^0 modes are

$$\frac{\mathcal{B}(B^0 \rightarrow J/\psi K_1^0(1270))}{\mathcal{B}(B^+ \rightarrow J/\psi K^+)} = 1.42 \pm 0.42 \quad (K^+ \pi^- \pi^0 \text{ mode})$$

$$\frac{\mathcal{B}(B^0 \rightarrow J/\psi K_1^0(1270))}{\mathcal{B}(B^+ \rightarrow J/\psi K^+)} = 1.07 \pm 0.45 \quad (K^0 \pi^+ \pi^- \text{ mode}),$$

where only statistical errors are shown [11]. Since the results for the two modes are consistent within errors, we combine the two data sets. The branching fraction ratios for the B^0 and B^+ are:

$$\frac{\mathcal{B}(B^0 \rightarrow J/\psi K_1^0(1270))}{\mathcal{B}(B^+ \rightarrow J/\psi K^+)} = 1.30 \pm 0.34 \pm 0.28$$

$$\frac{\mathcal{B}(B^+ \rightarrow J/\psi K_1^+(1270))}{\mathcal{B}(B^+ \rightarrow J/\psi K^+)} = 1.80 \pm 0.34 \pm 0.34,$$

where the first errors are statistical and the second are systematic. The absence of any signal in the $B^+ \rightarrow J/\psi K_1^+(1400)$ channel translates to a 90% confidence level limit on the branching fraction ratio of

$$\frac{\mathcal{B}(B^+ \rightarrow J/\psi K_1^+(1400))}{\mathcal{B}(B^+ \rightarrow J/\psi K_1^+(1270))} < 0.30.$$

The largest component of the systematic error ($\pm 14\%$) is due to errors in the $K_1(1270)$ branching fractions to the $K\pi\pi$ modes that are used for this measurement. We also include in the systematic error the level of possible contributions from other $K\pi\pi$ resonances ($\pm 9\%$) and non-resonant $K\pi\pi$ production ($\pm 7\%$), uncertainties in the relative $J/\psi K\pi\pi$ and $J/\psi K^+$ acceptance ($\pm 5\%$ for the B^+ channel and $\pm 10\%$ for B^0) and, for the B^0 , the uncertainty in the ratio of charged to neutral B meson production at the $\Upsilon(4S)$ ($\pm 8\%$) [12].

Since the $B \rightarrow J/\psi K^0 \pi^+ \pi^-$ decays proceed primarily via the *flavor-nonspecific* $K^0 \rho^0$ intermediate state, they are potentially useful for CP violation studies. In principle, these final states are mixtures of $CP = \pm 1$ eigenstates, depending on the orbital angular momentum of the J/ψ and the K_1 . With sufficient statistics, the relative strengths of the two CP eigenstates can be determined from an analysis of final state helicity angle distributions [13]. The situation is made complicated by possible interference between the $K^0 \rho$ amplitude and those for $K^* \pi$ and $K_0^*(1430) \pi$. Theoretical work is needed to clarify the situation.

In summary, we report the first observation of the $B \rightarrow J/\psi K_1(1270)$ decay mode. Using the PDG value of $\mathcal{B}(B^+ \rightarrow J/\psi K^+) = 1.00 \pm 0.10 \times 10^{-3}$ [8], we translate our measurements into the branching fractions:

$$\mathcal{B}(B^0 \rightarrow J/\psi K_1^0(1270)) = (1.30 \pm 0.34 \pm 0.31) \times 10^{-3}$$

$$\mathcal{B}(B^+ \rightarrow J/\psi K_1^+(1270)) = (1.80 \pm 0.34 \pm 0.39) \times 10^{-3}.$$

These measurements indicate that this mode constitutes a reasonable portion ($\sim 15\%$) of the total number of $B \rightarrow$

$J/\psi X$ decays. We see no evidence for $B \rightarrow J/\psi K_1(1400)$ and set an upper limit for this decay branching fraction.

We wish to thank the KEKB accelerator group for the excellent operation of the KEKB accelerator. We acknowledge support from the Ministry of Education, Science, Sports and Culture of Japan and the Japan Society for the Promotion of Science; the Australian Research Council and the Australian Department of Industry, Science and Resources; the Department of Science and Technology of India; the BK21 program of the Ministry of Education of Korea, CHEP SRC program of the Korea Science and Engineering Foundation and Creative Research Initiative program of the Ministry of Science and Technology of Korea; the Polish State Committee for Scientific Research under contract No.2P03B 17017; the Ministry of Science and Technology of Russian Federation; the National Science Council and the Ministry of Education of Taiwan; the Japan-Taiwan Cooperative Program of the Interchange Association; and the U.S. Department of Energy.

-
- [1] D. Bortoletto *et al.* (CLEO Collab.), Phys. Rev. **D45**, 21 (1992); H. Albrecht *et al.* (Argus Collab.), Phys. Lett. **B199**, 451 (1987). Both papers quote branching fractions for $B^+ \rightarrow J/\psi K^+ \pi^+ \pi^-$ based on $3 \sim 5$ signal events.
 - [2] K. Abe *et al.* (Belle Collab.), *The Belle Detector*, KEK Report 2000-4, to be published in Nucl. Instr. and Meth.
 - [3] KEKB B Factory Design Report, KEK Report 95-1, 1995, unpublished.
 - [4] Events are generated with the CLEO group's QQ program (www.lns.cornell.edu/public/CLEO/soft/qq); the detector response is simulated using GEANT, R. Brun *et al.*, GEANT 3.21, CERN Report DD/EE/84-1, 1984.
 - [5] The negative ΔE region contains events from $B \rightarrow J/\psi K \pi \pi X$ where X is a low energy pion or photon that is not included in the M_{bc} and ΔE computation. Therefore, we do not use this region for sideband studies and exclude the $\Delta E < -0.1$ GeV region from the fits shown in Fig. 2.
 - [6] The limited phase space for the $K_1(1270) \rightarrow K \rho$ decay results in an asymmetric $\rho \rightarrow \pi\pi$ line shape.
 - [7] W. M. Dunwoodie, private communication. The function is a convolution of an S-wave Breit Wigner function with mass and width fixed at the PDG values for the $K_1(1270)$ with a P-wave Breit Wigner function for the ρ meson.
 - [8] D.E. Groom *et al.* (PDG), Eur. Phys. Jour. **C15**, 1(2000).
 - [9] The range of the fit is restricted to $M_{K\pi\pi} < 1.7$ GeV because of possible contributions from higher mass $K\pi\pi$ states.
 - [10] A. Abashian *et al.* (Belle Collab.), Phys. Rev. Lett. **86**, 2509 (2001).
 - [11] Statistical errors include the errors on the numbers of signal and $J/\psi K^+$ events from the fits and the MC-statistics

component of the acceptance error added in quadrature.

[12] J.P. Alexander *et al.* (CLEO Collab.), Phys. Rev. Lett. **86**, 2737 (2001).

[13] The situation is somewhat analogous to that for $B \rightarrow J/\psi K^*$, as discussed, for example, in I. Dunietz *et al.*, Phys. Rev. **D43**, 2193 (1991).

TABLE I. Results of the fits to the M_{bc} and ΔE projections.

Channel	N_{evts}
$J/\psi K^+ \pi^+ \pi^-$	53.4 ± 9.1
$J/\psi K^+ \pi^- \pi^0$	19.3 ± 5.1
$J/\psi K^0 \pi^+ \pi^-$	6.2 ± 2.6
$J/\psi K^+$	472.4 ± 22.9

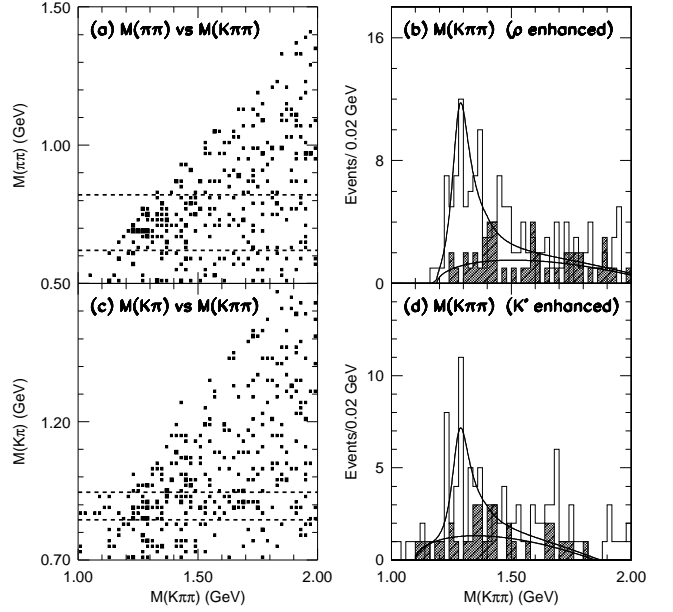


FIG. 1. (a) The distribution of $M_{\pi^+\pi^-}$ vs $M_{K^+\pi^+\pi^-}$ for $B \rightarrow J/\psi K \pi \pi$ candidates. The dashed lines indicate the $\rho \rightarrow \pi\pi$ selection region. (b) The $K\rho$ mass distribution for the signal (clear histogram) and sideband (cross-hatched histogram) regions. (c) $M_{K\pi}$ vs $M_{K^+\pi^+\pi^-}$ for the same events. The dashed lines indicate the $K^* \rightarrow K\pi$ selection region. (d) The $K^*\pi$ mass distribution for the signal (clear histogram) and sideband (cross-hatched histogram) regions. The curves are the results of the fits described in the text.

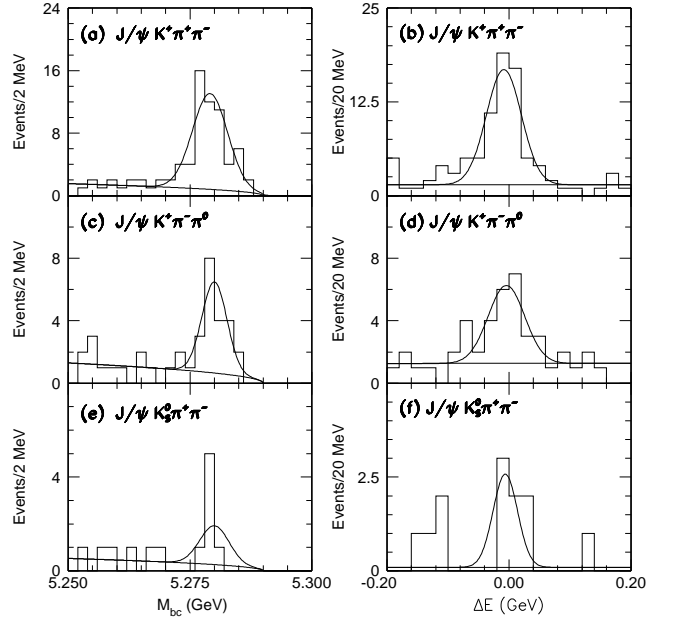


FIG. 2. (a) The M_{bc} and (b) ΔE projections for the $K^+ \pi^+ \pi^-$ channel. The fits are described in the text. The corresponding distributions and fits for the $K^+ \pi^- \pi^0$ and $K_S^0 \pi^+ \pi^-$ channels are also shown.